

Charge Separation in Intermixed Polymer:PC₇₀BM Photovoltaic Blends: Correlating Structural and Photophysical Length Scales as a Function of Blend Composition

Hendrik Utzat^{1,2}, Stoichko D. Dimitrov^{1,3*}, Scot Wheeler¹, Elisa Collado-Fregoso¹, Pabitra Shakya Tuladhar¹, Bob C. Schroeder^{1,4}, Iain McCulloch^{1,5} and James R. Durrant^{1,3*}

¹ Centre for Plastic Electronics, Department of Chemistry, Imperial College London, Exhibition Road, London SW7 2AZ, UK

² Massachusetts Institute of Technology, Department of Chemistry, 77 Massachusetts Avenue, Cambridge, Massachusetts 02139, United States

³ SPECIFIC, College of Engineering, Swansea University, Bay Campus, Swansea SA1 8EN, UK

⁴ Department of Chemical Engineering, Stanford University, 443 Via Ortega, Stanford, California 94305, United States

⁵ SPERC, Physical Sciences and Engineering Division, King Abdullah, University of Science and Technology (KAUST), Thuwal 23955_6900, Saudi Arabia.

Abstract

A key challenge in achieving control over photocurrent generation by bulk-heterojunction organic solar cells is understanding how the morphology of the active layer impacts charge separation and in particular the separation dynamics *within* molecularly-intermixed donor-acceptor domains versus the dynamics *between* phase-segregated domains. This paper addresses this issue by studying blends and devices of the amorphous silicon-indacenodithiophene polymer SiIDT-DTBT and the acceptor PC₇₀BM. By changing the blend composition, we modulate the size and density of the pure and intermixed domains on the nanometre lengthscale. Laser spectroscopic studies show that these changes in morphology correlate quantitatively with the changes in charge separation dynamics on the

nanosecond timescale, and with device photocurrent densities. At low fullerene compositions, where only a single, molecularly intermixed polymer-fullerene phase is observed, photoexcitation results in a ~30% charge loss from geminate polaron pair recombination, which is further studied via light intensity experiments showing that the radius of the polaron pairs in the intermixed phase is 3-5 nm. At high fullerene compositions ($\geq 67\%$), where the intermixed domains are 1-3 nm and the pure fullerene phases reach ~4 nm, the geminate recombination is suppressed by the reduction of the intermixed phase making the fullerene domains accessible for electron escape.

1. Introduction

Organic solar cells (OSC) have been reported with power conversion efficiencies exceeding 10 %, ¹⁻³ making them a promising third-generation photovoltaic technology. The photoactive layer of a typical OSC is a blend of a conjugated polymer and the derivative of the fullerene C₆₀ (PC₆₀BM) or the less symmetrical C₇₀ (PC₇₀BM). Photoexcitation of these blends results in photoinduced charge separation between the polymer and fullerene, and charge transportation to the device electrodes. Whilst early models of device function employed structural pictures of the photoactive layer based on the formation of well defined, and chemically pure, polymer and fullerene phases, it is now understood that many donor polymers are highly miscible with fullerenes, forming complex film structures in which pure polymer and/or fullerene phases co-exist with a molecularly intermixed polymer-fullerene phase. ⁴⁻⁹ Such complex, but more realistic, structural models are motivating studies of the correlations between film morphology and the processes of charge generation and device function in OSC. ^{6,8,10-19} In this study, we address this issue for blend films and devices employing an amorphous donor polymer silindacenodithiophene donor (SiIDT-DTBT) previously shown to exhibit high miscibility with PC₆₀BM. ²⁰ Our study employs a range of blend ratios to modulate the blend morphology and both rigorous structural and spectroscopic characterization allowing us to quantitatively analyse the correlations between blend structure and device performance.

Charge photogeneration in OSC is the process of formation of dissociated, coulombically unbound electrons and holes that can freely move through the film generating photocurrent. Charge generation is initiated by light absorption by the polymer and/or the fullerene, forming singlet excited states (called

excitons) exhibiting finite diffusion lengths of typically 3-10 nanometres.^{21,22} This exciton diffusion length imposes a severe limit on the maximum lengthscale of polymer -fullerene phase separation in the blend film for efficient exciton dissociation. For example, for an exciton diffusion length of 5 nm, requiring 90% of excitons to reach a donor: acceptor interface implies a diffusion length of ~ 1.6 nm, or pure domain diameter of ~ 3.2 nm. For some crystalline donor polymers, such as P3HT and DPP-based polymers, blend films exhibit relatively modest polymer photoluminescence (PL) quenching (60 - 80 %), indicative of the formation of pure polymer domains on lengthscales approaching exciton diffusion lengths.^{23,24} However, most polymer:fullerene blends employed in efficient OSC show very high polymer PL quenching yields (>95%), indicative of very efficient polymer exciton dissociation in a polymer: fullerene phase intermixed on a molecular lengthscale of < 1 - 2 nm.²⁵ Given that in most (but not all) blend films, polymer light absorption is responsible for most photocurrent generation, such intermixed domains will play a key role in photocurrent generation, as has been suggested in recent studies.^{5,10,26} It is important to note that such short lengthscales start to approach the diameter of individual PC₇₀BM molecules (~ 1 nm) and the monomer repeat unit length (and exciton wavefunction delocalisation length) of many donor polymers.^{22,27,28} A further consideration for charge separation in such blend films is coulomb attraction of photogenerated electrons and holes after exciton dissociation, which can result in the formation of bound electron-hole pairs. The coulomb capture radius of such electron-hole pairs is typically estimated in the range of 2 - 20 nm (depending upon definition and means of calculation / measurement), of a similar or longer lengthscale than the lengthscale of phase segregation in the blend film.^{12,29,24} Unravelling these overlapping lengthscales, and their impact on device performance, is therefore a significant challenge, and the key focus of this manuscript.

Charge recombination losses following exciton dissociation play a key role in limiting OSC device efficiency.^{11,30,31} Taking place primarily in the photoactive layer, these can be classified as either geminate recombination, typically associated with recombination of bound electron-hole pairs, and non-geminate recombination of dissociated charges; both are thought to be strongly dependent on film nanomorphology.^{10,32} For example, recent ultrafast transient absorption spectroscopy (TAS) studies and theoretical calculations have provided evidence that efficient charge generation and dissociation (i.e.: generating spatially uncorrelated electrons and holes) is associated with the tendency of PC₆₀BM

to form pure,^{17,33,34} aggregated domains in most polymer:fullerene blend films with a PCBM content above the 'miscibility' threshold.^{6,10,29} Such pure PCBM domains have been suggested to provide a high density of highly delocalised acceptor states, allowing ultrafast electron delocalisation aiding successful electron-hole dissociation.^{35,36} Aggregation has also been suggested to increase the PCBM electron affinity, creating an additional energetic offset to aid charge separation.^{10,29} Analogous energetic shifts have been reported for polymer aggregation / crystallisation.³⁵ Recent Monte Carlo simulations have provided a theoretical framework for such observations, suggesting that the energetic offsets between pure (aggregated) and mixed (amorphous) domains, as well as local energetic disorder, may aid the dissociation of coulombically attracted electron-hole pairs.^{29,32}

In this study, we therefore investigate the relationship between photocurrent generation and film structure on the nanometre length scale in the polymer:fullerene pair of silindacenodithiophene (SiIDT-DTBT): PC₇₀BM. SiIDT-DTBT (see figure 1) is representative of a range of relatively amorphous indacenodithiophene based polymers which have been shown to be highly miscible with PC₇₀BM, while still sustaining efficient photocurrent generation in optimal, typically 1:3, blend compositions.²⁰ In the present study, blends with different compositions were fabricated to allow us to study the impact of film nano-structure on the charge generation dynamics. In particular, employing this approach, we investigate whether photophysical descriptions of charge separation determined the highly crystalline model blend system pBTTT:PCBM^{15,17,37-39} can be extended to an amorphous blend more representative of many technologically relevant OPV blends, and determine in particular the relevant structural and photophysical length scales in this amorphous blend which determine the efficiency of charge separation. Using a combination of electron microscopy and photoluminescence spectroscopy we identify that this material system forms a single polymer:fullerene phase in the blends with low fullerene composition and a mix of pure fullerene and intermixed polymer:fullerene phases in the blends with excess fullerene. Time-resolved spectroscopy of films and devices reveal that initial electron transfer is independent of the structure of the films and it takes place primarily within the intermixed polymer:fullerene phase on a sub-picosecond timescale. Geminate charge recombination on the nanosecond timescale is however highly sensitive to the structure of the films. Its suppression requires the formation of fullerene aggregates within the Coulomb capture radius of the blend

(estimated herein to be approximately 3-5 nm) providing an energy landscape for efficient electron migration away from the hole. At sub-optimal PC₇₀BM compositions, whilst efficient charge collection is still possible under strong reverse voltage bias both geminate and non-geminate charge recombination severely limit photocurrent generation under short circuit conditions.

2. Results

2.1. Morphology of SiIDT-DTBT:PC₇₀BM blends

Figure 1a presents the TEM images of spin-coated SiIDT-DTBT:PC₇₀BM blend films with 1:1, 1:2 and 1:4 polymer:fullerene weight ratios. A clear evolution in the structure of the films is seen with the addition of excess fullerene to the blend. The TEM image of the 1:1 blend appears mostly uniform, indicating the film is dominated by one highly-intermixed polymer-fullerene phase rather than a mix of phase separated polymer and fullerene phases. This result is consistent with the highly amorphous nature of SiIDT-DTBT, which shows no clear signatures of pi-pi or lamellar stacking in wide-angle X-ray scattering measurements of un-annealed as cast films.²⁰ The TEM images of the 1:2 and 1:4 blends are however much coarser, consisting of contrasting dark and bright patches, indicating the separation of fullerene-rich domains (dark areas) out of the intermixed phase.⁴⁰ The fullerene domains appear with approximate diameters of ~ 1.7 nm and 4 nm in the 1:2 and 1:4 blend respectively (as estimated from the TEM images). These fullerene domains appear embedded with a paler regions assigned to the intermixed phase, with the widths of these intermixed regions being approximately ~ 3 nm and ~ 1 nm for the 1:2 and 1:4 blends respectively. The mixed domain appears more interconnected through the film.

Photoluminescence quenching was used as a further probe of blend morphology. Figure 1b compares the relative photoluminescence intensities of five SiIDT-DTBT:PC₇₀BM blends with 4:1, 2:1, 1:2, 1:4 and 1:10 weight ratios after film excitation at 510 nm, as well as neat SiIDT-DTBT and PC₇₀BM films. The absorption of the films agrees with previously published spectra and is included in the supporting information (SI).²⁰ The SiIDT-DTBT photoluminescence is very strongly quenched in all blends reaching ~ **98 %** for the 4:1 blend and > **99%** for all others. Such high yields of quenching are consistent with the morphological picture built by our TEM analysis and confirms that SiIDT-DTBT and

PC₇₀BM are highly miscible and tend to form an intimately mixed polymer:fullerene phase instead of pure polymer domains even in blends with 80 % polymer.

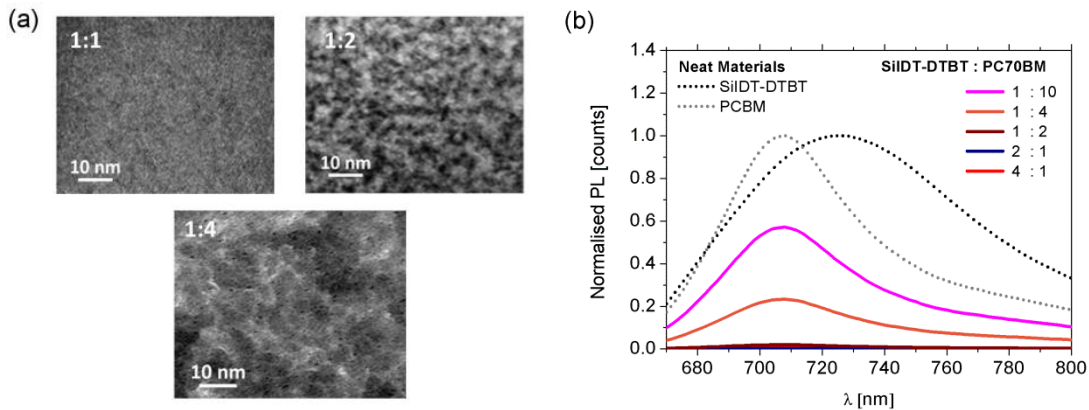


Figure 1: (a) Representative TEM images of the SiIDT-DTBT: PC₇₀BM blends with 1:1, 1:2 and 1:4 compositions, at which the appearance of pure fullerene domains is observed. **(b)** Normalized photoluminescence spectra of five SiIDT-DTBT: PC₇₀BM blends excited at 510 nm. The emission of PC₇₀BM is corrected for light absorption at the excitation wavelength. SiIDT-DTBT emission is included as a reference.

In contrast to the high polymer emission quenching, the PC₇₀BM emission is only fully quenched in the polymer-rich 4:1 and 2:1 blends. More modest fullerene PL quenching is observed in the 1:2 blend, whilst the fullerene-rich 1:4 and 1:10 blends show strong fullerene emission. These reductions in fullerene PL quenching coincide with the appearance of detectable pure fullerene domains in the TEM images of the 1:2 and 1:4 blends (Figure 1b). These PL quenching data allows us to approximate the size of the PC₇₀BM-rich domains by using a simple model based on PC₇₀BM exciton diffusion in a pure spherical domain with quenching at the domain interface.¹⁰ Assuming a unity quantum yield of the fullerene exciton quenching at the fullerene/polymer interface, we can use the equation $L = L_{EX} (1 - PLQ)^{1/2}$ to estimate the radius of the PC₇₀BM domains. Here, L is the mean distance the exciton travels before quenching; PLQ is the photoluminescence quenching yield and L_{EX} is the fullerene exciton diffusion length. We use the known diffusion length of PCBM excitons of 3.2 - 5 nm, determined experimentally with time-resolved laser spectroscopic techniques.^{41,42} Using this analysis, we obtain L values of 1.8 - 2.9 nm in the 1:4 film and 1.0 - 1.5 nm in the 1:2 film, indicating pure fullerene domain diameters of 3.6 - 5.8 nm in the 1:4 blend and 2 - 3 nm in the 1:2 blend. Table 1

summarizes the results from the PL and the TEM analysis of the domain sizes, which show good agreement between these two measurements. In summary, we conclude that the SiIDT-DTBT: PC₇₀BM blends with high polymer-loading consist of a single intermixed polymer:fullerene phase, whilst the blends with excess fullerene consist of two coexisting phases that are a pure fullerene and a finely intermixed polymer-fullerene phase.

Polymer/PCBM blend ratio	Intermixed phase width from TEM [nm]	PCBM Domain size from PLQ [nm] ^(a)	PCBM domain size from TEM [nm]
4:1	n/a	<1	n/a
2:1	n/a	<1	n/a
1:1	continuous	<1	<1
1:2	3.1 ± 1	2-3	1.7 ± 1
1:4	~1	3.6-5.8	4.0 ± 1
1:10	n/a	4.6-7.6	n/a

Table 1. Domain widths (diameters) of PCBM and intermixed phases estimated from TEM and PL results. ^(a) employing 3.1 - 5 nm PCBM exciton diffusion length.

2.2. Exciton dynamics and charge generation

Ultrafast transient absorption spectroscopy (TAS) was used to investigate the impact of film morphology on the excited state dynamics in the SiIDT-DTBT:PC₇₀BM 4:1, 2:1, 1:2 and 1:4 blends and a neat SiIDT-DTBT film. Representative transient absorption spectra of the SiIDT-DTBT film and the 4:1 blend film are presented in **Figure 2a** and **Figure 2b**, respectively. All data were collected with an excitation at 630 nm, which corresponds to the maximum of the polymer absorption, in order to study the charge generation dynamics from SiIDT-DTBT excitons. The neat SiIDT-DTBT film shows a broad excited state absorption peak with a maximum at ~1200 nm which we assign to singlet exciton absorption, because of its short lifetime (30 ps half-life) and ample literature assigning these type of NIR signals to polymer singlet excited states.⁴³ Residual photoinduced absorption with a maximum at ~1050 nm is also observed in the spectra at longer time delays, matching the absorption of the triplet exciton of SiIDT-DTBT recorded using microsecond transient absorption spectroscopy.⁴⁴ We hence identify that the polymer singlet exciton can undergo intersystem crossing to the triplet manifold.

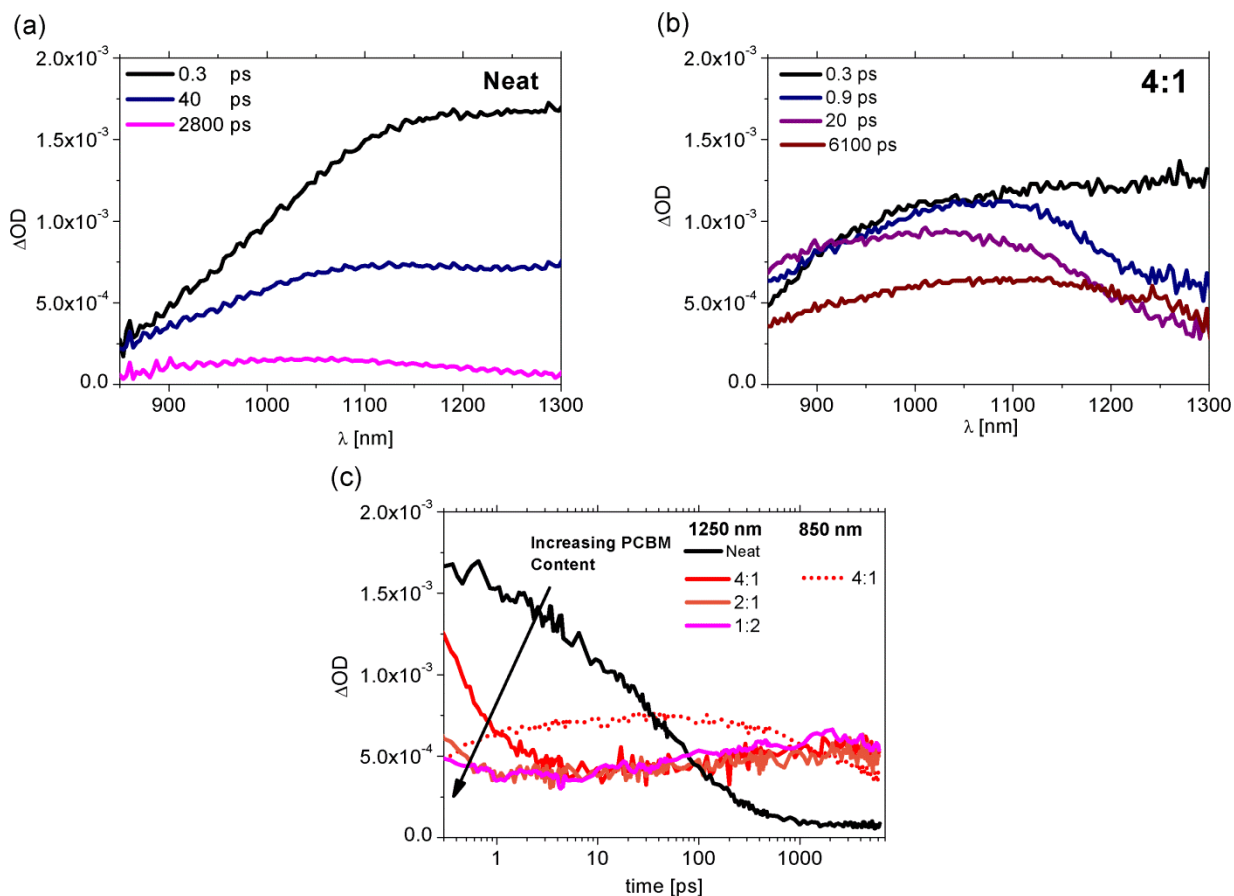


Figure 2: Transient Absorption Spectra at different times after photoexcitation of **(a)** neat SiIDT-DTBT and **(b)** 4:1 SiIDT-DTBT:PC₇₀BM blend. **(c)** Single wavelength kinetics of the neat SiIDT-DTBT and the 4:1, 2:1, 1:2 and 1:4 SiIDT-DTBT:PC₇₀BM blends excited at the maximum of the polymer absorption band at 630nm with $6 \mu\text{Jcm}^{-2}$ and probed at 1200 nm. The 850 nm kinetic of the 4:1 blend is also included to the graph to show the growth of the polaron signal simultaneously with the decay of the polymer singlet exciton. All spectra and traces were normalized for film absorption at the excitation wavelength.

In the first picosecond after excitation, the TA spectrum of the 4:1 blend in Figure 2b evolves from polymer exciton-like into a new absorption spectrum that has a band centred at ~ 1000 nm. This is then followed by peak shifting from 1000 nm to 1150 nm in the following nanosecond. We assign the first spectral evolution to the dissociation of the polymer exciton via electron transfer, which leads to the formation of an electron on PC₇₀BM and a hole on the polymer; thus the 1000 nm band is assigned to polymer hole polaron absorption. The subsequent red-shift of this band may be explained by polaron

thermalisation within the hole density of states.^{45,46} Based on the peak positions of the initial and relaxed hole polarons, we calculate a relaxation energy of ~160 meV suggesting significant disorder in the blend, as expected for the films of the relatively amorphous SiIDT-DTBT. A similar degree of disorder (~70 meV) has been observed for the likewise amorphous PCDTBT:PCBM system⁴⁷

Figure 2c shows the transient absorption dynamics for the 4:1 blend at two representative wavelengths: 1250 nm – dominated by polymer exciton absorption in the first picosecond then by the weaker polaron absorption at longer times, and 850 nm – where the polaron absorption exceeds that of the singlet exciton. The 1250 nm signal exhibits a rapid exponential decay phase with a half-time of 0.5 ps, which correlates with a similarly rapid rise of the polaron signal at 850 nm. We assign this signal dynamics to electron transfer from SiIDT-DTBT singlet excitons to PC₇₀BM. This decay is 60 times faster than the 30 ps decay observed for the neat SiIDT-DTBT films and it is therefore in excellent quantitative agreement with our PL quenching estimate (98%) for this blend composition. We note that the initial transient absorption at 1250 nm in the 4:1 blend is only ~ 20% lower than the absorption of the exciton in neat SiIDT-DTBT, suggesting only a small contribution of faster carrier generation within our instrument response (200 fs). We also add that the apparent nanosecond rise in the 1250 nm kinetic corresponds to spectral red-shifting due to polaron relaxation rather than any polaron generation, as discussed in the previous paragraph. This signal red-shifting is also observed for all blend compositions.

In addition to the kinetics of the 4:1 blend, **Figure 2c** includes the transient absorption decay at 1250 nm for the other three studied blends of SiIDT:DTBT:PC₇₀BM: 2:1, 1:2 and 1:4. We can thus compare the timescales of exciton dissociation as a function of film morphology. While the SiIDT-DTBT exciton in the 4:1 blend decays with a 0.5 ps time constant, the lifetime of the polymer exciton in the 2:1 blend is significantly shortened, limited by our instrument response (200 fs). The fullerene-rich 1:2 blend only shows a minor singlet exciton feature decaying on a sub-picosecond timescale, suggesting that for this blend the electron transfer is mostly completed within 200 fs, too. This result is congruent with numerous studies of other polymer:fullerene systems also showing ultrafast charge generation.^{33,47} This decrease of the time constant of electron transfer is consistent with previously observed results

for PCDBT:PCBM blends⁴⁸ and can be explained with slightly delayed exciton diffusion limited electron transfer in the 4:1 blend and perhaps in the 2:1 blend, and matches the morphological picture built by our PL and TEM results.

2.3. Geminate Charge Recombination Dynamics

According to **Figure 2 c** the electron transfer from polymer excitons is a fast process with a near unity efficiency (> 98 %) for all SiIDT-DTBT:PC₇₀BM blends. It can be considered as essentially independent of film morphology from the prospective of overall photocurrent generation yields, as the difference in exciton quenching between different compositions is just 2 %. In this section, we focus on the dynamics of photogenerated charges after the completion of the electron transfer process. We therefore recorded the polaron decay dynamics of the 4:1 blend as a function of light intensity (Figure 3 a) and the 4:1, 2:1, 1:2 and 1:4 blends as a function of film composition (Figure 3 b). All kinetic traces represent the integrated polaron signals from 10 ps to 6 ns time delays. The integration was performed in the accessible 850 – 1400 nm spectral range to more accurately assess the hole recombination dynamics between the different blends.⁴⁹

Figure 3 a presents the time trace of the integrated differential absorption in the 4:1 blend recorded at 4 different light excitation intensities, corresponding to initial exciton densities between $2.2 \cdot 10^{17} \text{ cm}^{-3}$ and $122 \cdot 10^{17} \text{ cm}^{-3}$. These correspond to average singlet exciton separations of 17 nm for the lowest excitation intensity and 4.4 nm for the highest excitation intensity, assuming a uniform distribution of the excitons in the film. The decay dynamics of this signal, assigned to the loss of polaron absorption due to charge recombination, is intensity independent for the two lowest excitation densities used, corresponding to exciton separation distances of 9.9 and 17 nm. This indicates that the observed polaron recombination is dominated by geminate electron-hole recombination at these light density levels. Our assignment to geminate recombination is further supported by our successful fitting of the polaron decay in Figure 4a with a single-exponential function, indicating a first order recombination dynamics. From the magnitude of the decay, we can estimate that this geminate charge recombination is responsible for ~30 % polaron signal loss in this 4:1 blend film. A further increase in the light excitation intensity (corresponding to singlet exciton separation of 5.5 nm) leads to strong reduction of

the polaron lifetime, assigned to the increasing dominance of non-geminate charge recombination on the polaron decay kinetics. Such fast non-geminate recombination is possible when more than one geminate electron-hole pair is generated within the volume of one bound pair. We can therefore estimate an effective radius for these bound electron-hole pairs of ~ 3 -5 nm (i.e. a diameter between the employed singlet exciton separations of 5.5 and 9.9 nm). This effective radius can be seen as the average carrier separation of dynamic electron-hole pairs over the timescales of geminate recombination.²⁹ Our value of this effective radius suggests that geminate electron-hole dissociation can be considered complete when the two charges are over 3 - 5 nm apart. We note that this electron-hole pair radius is of similar magnitude to estimates of the coulomb capture radius in such blends from a range of modelling and simulations studies.^{24,29,32,50-52}

Figure 3 b compares the polaron recombination dynamics of SiIDT-DTBT:PC₇₀BM as a function of blend composition, which allows us to study the impact of fullerene aggregation on the geminate recombination dynamics. The polaron decays were recorded for excitation densities that generated intensity independent signal decays. According to our results, the 4:1 and 2:1 blends show a similar level of signal loss due to geminate recombination that is 30 % at 6 nanoseconds. The blends with excess fullerene show much lower signal loss that accounts for 16 % for the 1:2 blend and 0% within our noise levels for the 1:4 blend. The corresponding time-constants of geminate recombination are 2.1 ± 0.1 ns for the 4:1 and 2:1 blends and of 1.8 ± 0.2 ns for the 1:2 blend estimated from single-exponential fitting of the kinetics (within the experimentally available time-range). This result indicates the strong impact of fullerene aggregation on the electron-hole polaron pair dissociation probability, leading to a near complete removal of the sub-6 ns geminate charge recombination losses in the high fullerene loading film of 1:4.

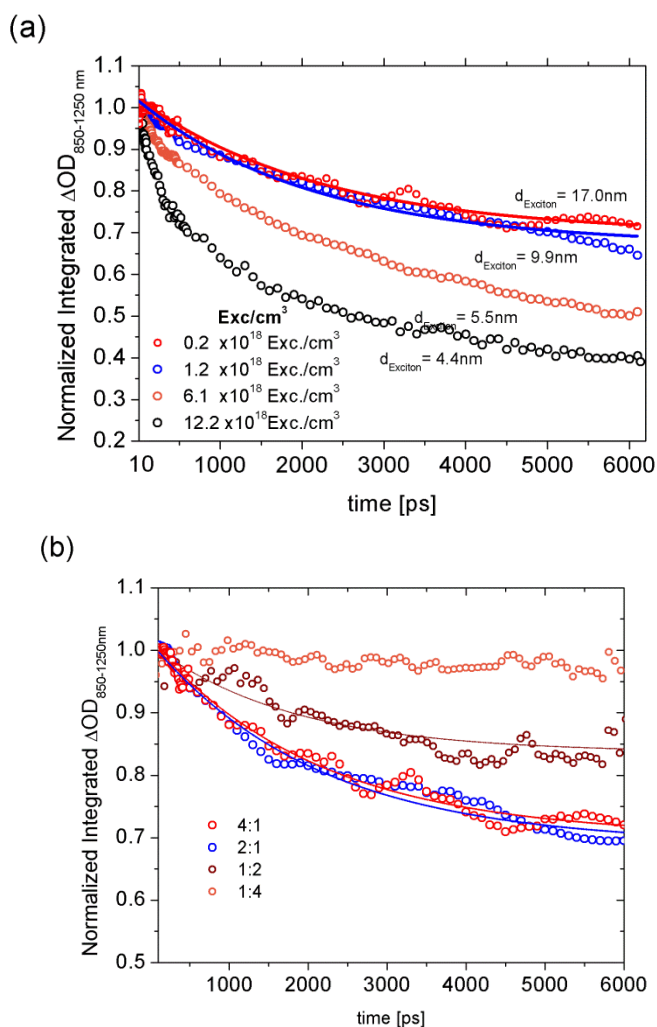


Figure 3: (a) Excitation fluence dependence of the decay of the hole polarons in the 4:1 blend. **(b)** Decay dynamics of the hole polarons for the SiIDT-DTBT:PC₇₀BM blends with different fullerene loading in the limit of low excitation fluences (1-6 $\mu\text{J cm}^{-2}$). The solid lines represent single-exponential fits to the experimental data.

2.4. Non-Geminate Carrier Recombination

Transient absorption spectroscopy on the microsecond timescale was carried out to analyse the non-geminate charge recombination losses in SiIDT-DTBT:PC₇₀BM films as a function of composition and light intensity. Single wavelength kinetics acquired at 850 nm are plotted in **Figure 4 a** for the 4:1, 2:1, 1:2 and 1:4 blends. They were successfully fitted with a power law function of the type, $OD = t^\alpha$ with $\alpha = -0.64$ to -0.39 providing evidence for trap-assisted bimolecular charge recombination in the films, typically observed for highly disordered semiconductors with an exponential charge trap state

distribution.⁵³ The 4:1 and 2:1 blends have almost identical recombination dynamics, whilst the 1:2 and 1:4 blends show a significant deceleration of the charge recombination. This observation is consistent with the expected impact of the addition of excess PC₇₀BM to the blends, leading to the formation of nanometre-sized PC₇₀BM aggregates which aid the spatial separation of electrons and holes and slow charge recombination.

The excitation intensity dependence of charge recombination is presented for the 1:10 blend composition, shown in **Figure 4 b**. At early times up to 2 μ s after photoexcitation, it is apparent that the kinetics become faster with increasing excitation density, assigned as previously to trap filling at high excitation densities, resulting in increased dominance of free carrier recombination. The recombination dynamics after 2 μ s are independent of excitation density, with the signal varying only in amplitude. Such dynamics are typical of trapping / de-trapping limited recombination.^{53,54}

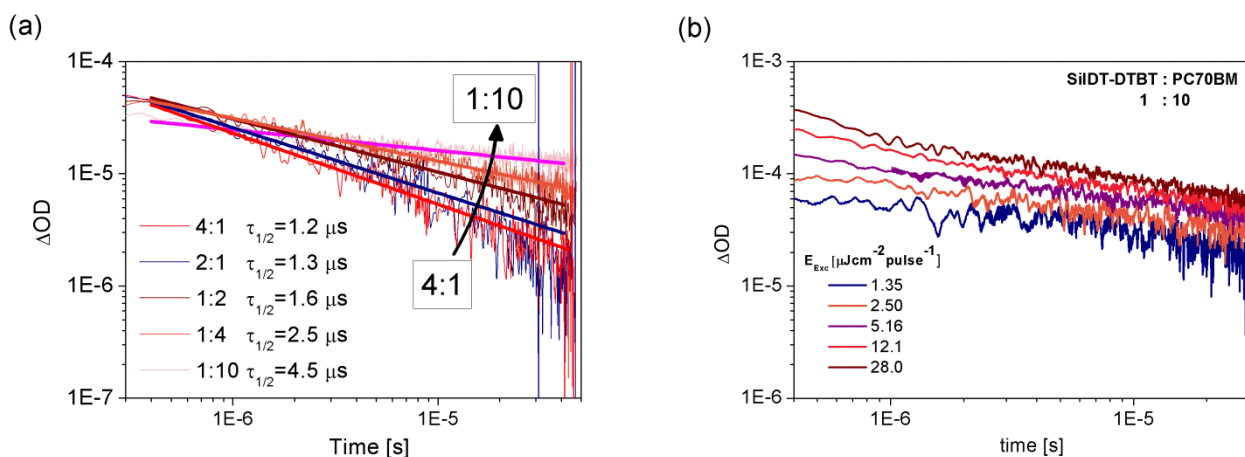


Figure 4: (a) Transient absorption decays on the μ s timescale of the SiIDT-DTBT: PC₇₀BM blends (4:1, 2:1, 1:2, 1:4 and 1:10). The traces are corrected for the film thickness to give a measure of the polaron density in the film. The solids lines represent power law fits to the dynamics. Signals were acquired at 850 nm after excitation of the polymer absorption band at 630 nm. The excitation fluence was adjusted for each film to generate near identical polaron densities. **(b)** Excitation fluence dependence of the recombination dynamics in the 1:10 blend recorded with a 630 nm excitation and probed at 850 nm.

2.5. Charge Dynamics and Device Performance

SiIDT-DTBT:PCB₇₀BM devices with four different blend ratios (4:1, 2:1, 1:2 and 1:4) were fabricated with standard ITO/PEDOT:PSS/Blend/Ca/Al architectures. The device J-V curves measured under simulated 1 sun AM1.5 conditions are included in the SI. The data show that the 1:4 blend is the most efficient device with a power conversion efficiency of 3.7 %, which is consistent with the reported efficiencies for SiIDT-DTBT:PC₇₀BM devices.²⁰ The photocurrent response of the devices with different composition were recorded under a wide range of applied bias, from -24 V to 1.5 V to study the effect of fullerene aggregation on the photocurrent generation properties of SiIDT-DTBT:PC₇₀BM. In order to allow for a direct comparison between our device photocurrent and TAS data, we used red light illumination spectrally centred at 630 nm, the excitation wavelength employed in our TAS experiments (spectrum shown in Figure S3).

Figure 5a presents the photocurrent densities generated by the devices under 630 nm excitation obtained after the subtraction of the devices' dark current. Very different bias dependent behaviour and photocurrent yields are observed between the devices with a different fullerene loading. The device short circuit currents (J_{SC}) vary widely between -1.1 mA cm⁻² for the 1:4 device and -0.06 mA cm⁻² for the 4:1 device. The generation of albeit small short circuit photocurrent by the 4-1 device indicates the possibility for charge extraction even from the highly intermixed polymer:fullerene blends. The blends with high fullerene loading show improved J_{SC} accompanied by an increase in device fill factor and open circuit voltage (V_{OC}) which are normally associated with slower non-geminate charge recombination due to the formation of electron percolation pathways. It is apparent that the corrected photocurrents of the fullerene-rich devices (1:2 and 1:4) are almost saturating at short circuit, and only increase slightly under reverse bias. In contrast, the high polymer loading (4:1 and 2:1) devices only exhibit significant photocurrents under a strong reverse bias, indicative of a requirement for strong electric fields to drive charge extraction on timescales fast enough to compete with non-geminate recombination.

In **Figure 5 b**, we compare the photocurrent densities generated by the SiIDT-DTBT:PC₇₀BM devices at short circuit (J_{SC}) and high reverse bias ($J_{ReverseBias}$) where a plateau region is reached. The device

data are plotted together with the temporal evolution of the polaron yields as received from our TAS results presented in **Figures 3 and 4**. The device photocurrent data are corrected for active layer absorption and PLQ and then normalised to the 1:4 blend; as such, the data points can be understood as relative internal quantum efficiencies with respect to the best 1:4 blend ($\text{IQE}_{\text{ReverseBias}}$). The device absorption at 630 nm was estimated from top electrode-free devices, and does not include possible contributions from interference effects (The polaron yield determined by TAS is also normalized to the 1:4 blend to allow the direct comparison of the TAS and device data as a function of blend composition. According to the results in **Figure 5 b**, $\text{IQE}_{\text{ReverseBias}}$ is, to a first approximation, independent of fullerene loading, thus suggesting that the device photocurrent generation at the plateau region (very high reverse bias) is very efficient for all blends and it is therefore independent of film morphology. This implies there is no need for pure fullerene domain formation for efficient charge generation to be achieved. This is in agreement with our ultrafast TAS results for the blend films. Furthermore, photogenerated carriers can be extracted in a highly efficient way under high reverse bias, even from highly intermixed device active layers. We note that due to approximate nature of this analysis, and the modest level of geminate losses even in the 4:1 blend, we cannot determine whether geminately bound carriers can be harnessed under strong reverse bias. The composition dependent polaron yields at long delay times (400 and 1500 ns) however show some correlation with the composition dependent evolution of the IQE_{SC} suggesting that device photocurrent densities at short circuit may correlate with this timescale polaron yields as estimate with TAS.^{55,56}

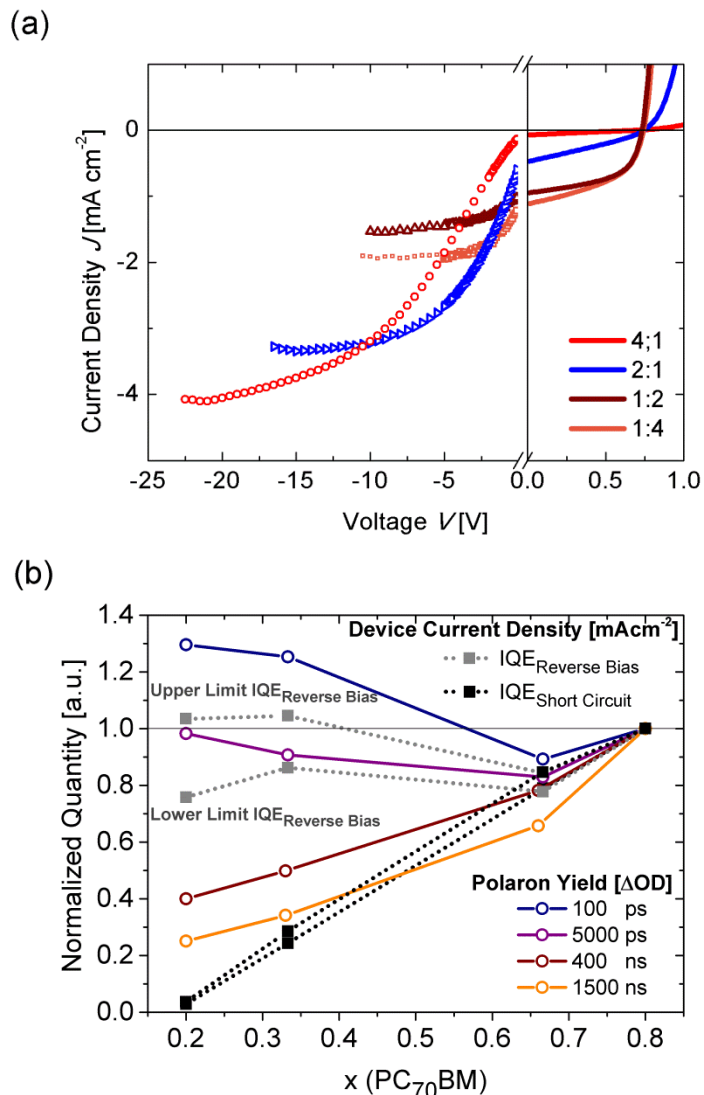


Figure 5: (a) Corrected photocurrent characteristics (-24V -0V, **scatter**) and standard JV curve (0-1.5V, **solid**) of different blend composition SiIDT-DTBT:PC₇₀BM devices under continuous red light illumination. (b) Correlation between hole polaron density as determined by TAS at different times after photoexcitation and device Internal Quantum Efficiencies under short circuit conditions (IQE_{Sc}) and strong reverse bias (IQE_{ReverseBias}) All quantities were corrected for the film absorption at 630 nm (the excitation wavelength in our TAS), losses due to PCBM exciton emission (only in 1:4 blend) and normalized to the 1:4 device. Care has been taken to minimize the differences between the initial carrier densities between different films and the microsecond and femtosecond measurements (SI, Table 2). To estimate the effect of electrode reflections, we calculated an upper limited of the IQE_{ReverseBias} (normalization by absorption times one) and a lower limit (normalization by the absorption times two).

3. Discussion

The spectroscopy and microscopy results presented herein allow us to develop a quantitative morphological picture of the SiIDT-DTBT:PC₇₀BM films on the nanometre length scale as a function of blend composition and relate it to the charge generation dynamics in the films. Based on these data, we can divide the blend films into two main categories as depicted in **Figure 6 a**. In the first category, for blends with less than 50 wt % of PC₇₀BM, we observe only one phase of highly intermixed polymer:fullerene molecules, whilst the second category for films with >50 wt % of PC₇₀BM, we observe two distinct film phases comprising a pure fullerene phase and intermixed polymer:fullerene phase. Such morphologies are expected for amorphous conjugated polymers like SiIDT-DTBT and have previously been reported for the popular PTB7 and PCDTBT polymers which are known to form polymer-fullerene blends with a very high degree of material mixing.⁸ In these films, pure fullerene phases appear at a certain miscibility threshold, above which fullerene domains can grow bigger than a few nanometres in diameter. The formation of pure, aggregated PCBM phases has been proposed to be a key factor in the separation of charges in such photovoltaic devices as it both increases the delocalisation of the fullerene acceptor states and provides an interfacial energy offset to stabilise charge separation.³⁴

In the intermixed phase, dominating the 4:1 blend, we find that the polymer PL quenching efficiency is > 98 %, in agreement with our TA assay of polymer singlet exciton decay dynamics. Assuming a typical polymer exciton diffusion length (L_{ex}) of 5 - 10 nm, this indicates an extremely short average diffusion distance for polymer excitons before meeting a fullerene of 0.7-1.4 nm. Assuming a uniform distribution within a single, molecularly intermixed phase, an average spatial separation of PC₇₀BM molecules in the film of ~ 3 nm can be estimated using typical polymer and fullerene densities (0.8 g / cm³ and 1.6 g / cm³ respectively). This implies that a polymer exciton would need to diffuse only 1.5 nm to be quenched by a fullerene (neglecting wavefunction delocalisation), which is in agreement with our estimate of the average polymer exciton diffusion distance estimated above. We note that even for this lowest fullerene composition blend, a 1.5 nm diffusion distance is similar to the length of 2 benzothiadiazole units along the polymer chain, and to the probable delocalisation of the polymer

exciton, as implied from TD-DFT calculations.⁴⁴ For higher fullerene compositions, we observe essentially instantaneous (< 200 fs) polymer exciton dissociation without any requirement for exciton diffusion. These results indicate that the fullerene composition in the intermixed domain is high enough such that photoexcitations always generate excitons effectively directly adjacent to a fullerene. They also show that charge generation can be efficient in intermixed polymer:fullerene phases without the presence of pure fullerene domains, which is consistent with the frequent reports of polymer:fullerene blends that exhibit very high polymer photoluminescence quenching yields (with the exception being blends with crystalline donor polymers which can exhibit large pure polymer domains).^{23,25,57,58} Overall, the presence of this molecularly intermixed phase ensures that dissociation of the polymer excitons is very efficient with an overall yield of >99 % for all the blends studied, except for the 4:1 where we estimate a minimal 2% loss.

In addition to a molecularly intermixed phase, the SiIDT-DTBT:PC₇₀BM films also form a second fullerene-rich phase at high fullerene blend compositions, as in the 1:2 and 1:4 blends studied herein. Our results and conclusions on the impact of this morphology change upon blend function are illustrated in figure 6. From the TEM and PLQ results summarised in Table 1, we estimate the diameter of the PC₇₀BM aggregates to be 4 - 6 nm in the 1:4 blend and 2 - 3 nm in the 1:2 blend. We observed from PLQ that the formation of such large fullerene domains results in a significant fullerene exciton decay to ground state during fullerene exciton diffusion, as illustrated in Figure 6a, corresponding to an ~ 20% loss of quantum yield for the 1:4 blend, which will result in some loss of photocurrent generation. Similar losses in the dissociation yields of the fullerene excitons have been reported previously and are understood in terms of diffusion limited exciton dissociation due to pure fullerene domain formation with sizes similar to or bigger than the fullerene exciton diffusion length, 3-5 nm.^{40,59} However, the presence of these domains also plays a key role in reducing geminate and non-geminate charge recombination losses within the blend, as we discuss below, such that optimum device performance is achieved at higher (1:3 or 1:4) blend ratios.

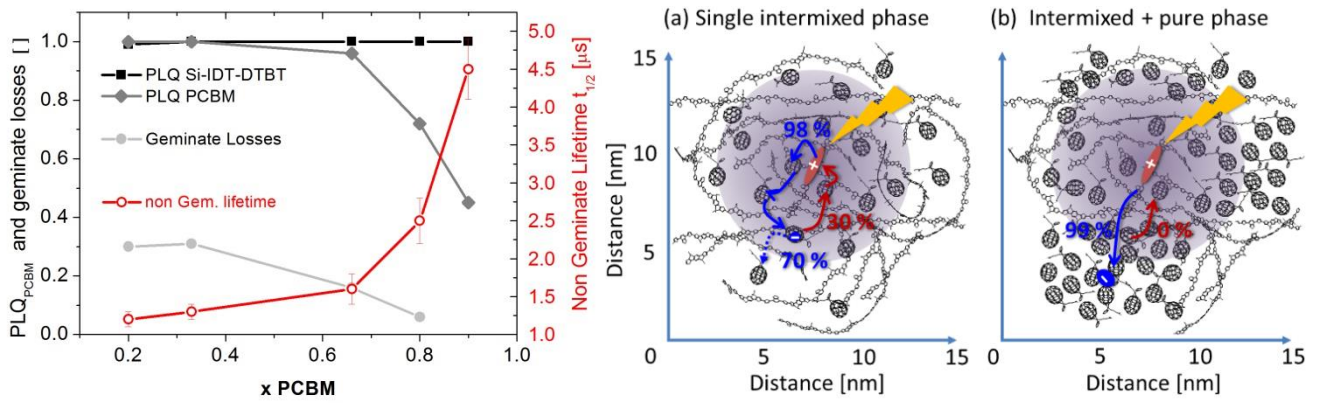


Figure 6: Summary of the blend composition dependence of the geminate losses, non-geminate recombination lifetimes and PLQ of the blend constituents as a morphological assay. **(a)** Schematic representation of the charge photogeneration and carrier recombination process in SiIDT-DTBT:PCBM devices of for a high polymer loading blend (left) and a high PCBM loading blend (right). Red represents hole density and blue electron density **(b)**.

After concluding that polymer excitons are efficiently separated in all SiIDT-DTBT:PC₇₀BM compositions, we focus on the impact of fullerene aggregation on the dissociation of the polarons generated by exciton separation, and in particular upon the role of this aggregation in reducing geminate and non-geminate recombination losses. From Figure 3 we find that intensity independent polaron recombination on the nanosecond timescale, assigned to geminate charge recombination is significant in blends lacking pure fullerene domains. However this geminate recombination loss pathway is composition dependent, leading to a 30% charge loss in the 4:1 and 2:1 blends, 16 % in the 1:2 blend and 0% in the 1:4 blend (Figure 6a). This result is in agreement with our recent report of field independent charge photogeneration in an operating SiIDT-DTBT:PC₇₀BM 1:3 device, and it shows that the formation of pure fullerene domains within the SiIDT-DTBT:PC₇₀BM intermixed phase has a strong impact on the charge separation dynamics of this polymer:fullerene blend. This result is also consistent with a recent report that in blends with the crystalline polymer PbTTT, fullerene aggregation can substantially suppress geminate recombination losses, and previous report that blends with higher fullerene composition exhibit a weaker requirement for a large LUMO level energy offset to avoid geminate recombination losses.^{60,61} We note that both theoretical and experimental studies have

demonstrated that fullerene aggregation can impact upon charge dissociation by creating an additional energy offset between pure and mixed domains due to well dispersed fullerenes have a 0.1 eV higher electron affinity than the aggregated fullerenes.¹⁰ In addition, such fullerene aggregation provides more delocalised electron states and a higher electron mobility to facilitate electron motion away from the fullerene.³⁴

Increased fullerene composition also correlates with slower non-geminate charge recombination and improved charge extraction. The retardation of non-geminate recombination with fullerene aggregation, as summarised in Figure 6a, most probably derives from the localisation of electrons in the aggregated fullerene domains due the increase in fullerene electron affinity with aggregation, thereby increasing the spatial separation of electrons and holes.²⁹ We note that at low fullerene compositions, charge collection at short circuit becomes very inefficient, both due to faster non-geminate recombination and most probably slower electron transport due to the absence of pure fullerene domains.^{11,62} In contrast, at strong reverse bias, charge collection becomes efficient independent of fullerene composition, indicating that strong electric fields can enable efficient charge extraction for all blends and consistent with our observation of efficient charge generation for all the blend compositions studied herein.

From our studies at low fullerene compositions, a key observation is that at high laser excitations densities, non-geminate recombination can become faster than geminate recombination. This allows us to estimate the average separation of the bound polaron pairs undergoing geminate recombination in the molecular intermixed phase to be 3-5 nm. It is apparent that that this distance is large enough such that several fullerenes reside in the volume spanned by each bound polaron pair, thus providing accessible electron accepting sites for random electron hopping during the lifetime of bound electron-hole pairs in the intermixed phase (and most likely for also analogous polymer polaron motion). The large average separation of these bound charges can be most obviously attributed to the balance between coulomb attraction, which will tend to pull the charges together, and local energetic inhomogeneities, which will tend to favour partial separation of the charges at local energetic minima. We note the behaviour of these geminate pairs is likely to evolve with time as the charges become increasingly trapped at these local energetic minima.

The size of the bound polaron pairs (3-5 nm) determined herein is large compared to the phase segregation length scales determined from our TEM and PL quenching data (intermixed region widths of 1-3 nm). As such, it can be concluded that geminate pairs generated in an intermixed phase do not need to diffuse as bound pairs within the mixed phase to access an interface with fullerene domains. Rather, at least for blend compositions $\geq 67\%$ fullerene, fullerene domains will be present within the diameter of such geminate pair, enabling these fullerene domains to directly aid the dissociation of these geminate pairs. This conclusion is consistent with the results of kinetic studies from the model blend system pBTTT:PCBM and P3HT:PCBM that the presence of fullerene aggregates suppresses geminate recombination,^{10,15,17,36-38} and indicates that the results obtained for this highly crystalline system, which forms polymer:fullerene co-crystals, can be extended to the more amorphous blends often employed in OPV devices. It is also consistent with the suppression of geminate recombination by these fullerene aggregates occurring directly upon polaron formation, without requiring a subsequent slow diffusion process, as recently concluded for the pBTTT:PCBM by Banerji et al.³⁷

Based on our morphological and functional data results, we can build a more complete picture of the charge separation dynamics in the amorphous blends studied herein, and in particular the impact of fullerene aggregation. This is summarised in Figure 6b where we distinguish between the two types of morphologies of the SiIDT-DTBT:PC₇₀BM blends: one with just an intermixed polymer:fullerene phase (the 4:1 blend) and another with both intermixed and pure phases (the 1:4 blend). These figures are drawn to scale based on our morphology analyses detailed above. The 3-5 nm radius of bound polaron pairs formed in the absence of aggregated fullerene domains is included as the shaded grey circle. In the 4:1 blend, photoexcitation results in both the generation of bound electron-hole pairs which undergo geminate recombination ($\sim 30\%$ yield) and the generation of dissociated charge carriers (the remaining 70%). This ability to generate dissociated charges (albeit with only a 70 % yield) in the absence of fullerene domains is most probably associated with the reasonably large energy offset ΔE_{CS} driving charge generation in this blend.^{30,63-65} However the absence of any phase structure to drive spatial separation of electrons and holes, and the absence of pure fullerene domains to facilitate rapid electron transport, these dissociated charges undergo relatively fast non-geminate recombination losses and a poor charge collection efficiency (except under strong reverse bias). The presence of

aggregated fullerene domains suppresses the formation of bound charge pairs and the resultant geminate recombination losses. Using our TEM analysis we estimate that the size of the intermixed phase in the 1:4 blend is ~1 nm, while the fullerene domains have an average diameter of ~ 4 nm. This means that in the 1:4 blend, experiencing no measurable geminate charge recombination losses, the size of the electron-hole pairs (generated by polymer excitons in the intermixed phase) extends over neighbouring pure fullerene domains. Considering these overlapping length scales, it is easy to understand that pure fullerene domains present in this blend, which provide both more delocalised electron acceptor orbitals and an increased electron affinity, are able to suppress the formation of bound polaron pairs and therefore prevent significant geminate recombination losses in this blend.

4. Conclusions

The photoactive films studied herein comprise blends of an amorphous 'push-pull' low bandgap polymer SiIDT-DTBT with the fullerene acceptor PC₇₀BM. Our TEM and PLQ morphology analyses indicates the presence of a singlet molecularly intermixed phase at low fullerene compositions, whilst at high fullerene compositions a biphasic morphology is observed with both an intermixed phase and pure fullerene domains. Exciton diffusion limitations within the pure fullerene domains provide a modest limitation on photocurrent generation from fullerene excitons. Efficient charge generation from polymer excitons is observed for all blend films studied, independent of the presence of aggregated fullerene domains. However, in the absence of pure fullerene domains, ~ 30 % of these photogenerated charges undergo geminate recombination. In addition, for these low fullerene content blends, efficient charge collection is only possible at strong reverse bias, attributed to faster non-geminate recombination and slower electron transport in the absence of pure fullerene domains. In bi-phasic blends with higher fullerene loadings, the presence of pure fullerene domains suppresses geminate recombination losses. This is attributed to the radius of bound polaron pairs, herein estimated to be 3-5 nm, being larger than the width of the intermixed regions (1 -3 -nm) such that all photogenerated electrons are able to directly access pure fullerene domains, facilitating their spatial separation from photogenerated holes. Our results therefore provide a clear picture of the impact of photocurrent generation in these blend films, with exciton dissociation occurring within molecular intermixed polymer / fullerene domains, but with the

presence of pure fullerene domains being critical to suppress both geminate and non-geminate recombination losses and to enable efficient charge extraction and device performance.

5. Experimental

Materials

The polymers studied here are synthesized by co-polymerization of SiIDT with and 4,7-di(thiophen-2-yl)-benzo[c][1,2,5]thiadiazole (DTBT) following published procedures.²⁰ The electron acceptor in this study is [6,6]-Phenyl-C₇₁-butyric acid methyl ester (PC₇₀BM) purchased from Sigma Aldrich.

OPV Device and Thin Film Preparation

ITO-coated glass substrates (Psiotec, 15 Ω sq⁻¹) were cleaned by successively sonicating in detergent DI water, DI water, acetone and iso-propanol. The substrates were then exposed to oxygen plasma cleaner (Diner Femto) for 7min. PEDOT:PSS (HC Starck, Baytron P Al 4083) was filtered through 0.45 μ m RC filter and deposited by spin-coating 3500 rpm, 30 s. The PEDOT/PSS layer was then annealed on a hotplate in air 150 ° C, 20 min.

The polymer SiIDT-DTBT and PC₇₀BM solutions were dissolved in chlorobenzene (>99%, Sigma Aldrich) with 25mg/ml. The different blend ratio solutions 4:1, 2:1, 1:2, 1:4 and 1:10 were prepared about an hour before spin coating by combining PC₇₀BM and SiIDT-DTBT solutions and vigorously stirring them. For devices, the blend solution was deposited onto PEDOT:PSS coated substrates in air by static spin-coating with 2500 rpm for 60 seconds. The devices were transferred in glove box for evaporation. Finally, Calcium (20nm) and Aluminium (100nm) was evaporated under vacuum 2.0×10^{-6} mbar, defining an active device area of 0.045 cm².

The films used for the spectroscopic studies were coated on glass substrates cleaned, treated and spin coated following exactly the same procedures as for the coating of the ITO glass substrates during device fabrication. The films for Transmission Electron Microscopy were prepared using a standard film floating technique.

Device Characterization

Devices J-V characteristics were tested by using Keithley 238 Source Measure Units. Illumination was provided using a 300 W xenon arc lamp solar simulator (Oriel Instruments) and calibrated using a silicon photodiode in order to ensure the illumination intensity of $100 \text{ mW} / \text{cm}^2$, at 1 sun AM 1.5. During the measurements, the devices were kept in nitrogen environment in a sealed chamber.

Corrected photocurrents were obtained from pulsed J-V measurements to minimize temperature differences in the light and dark, as well as device heating from possible large injection currents at far reverse bias.⁴⁴ The light source was integrated 1 sun equivalent provided by a ring of 11 white LEDs, which were pulsed by interrupting their power supply using a fast MOSFET switch; the light was on for 2 ms and off for 420 ms. For red light measurements the white LEDs were replaced with red LEDs with a maximum emission wavelength of 630 nm. The spectrum can be seen in the SI. The pulsed voltage source was provided by a Keithley 2400 SourceMeter and the current measured on a Tektronix TDS3032B oscilloscope across 50Ω .

Transient Absorption Spectroscopy

TAS measurements on the μs timescale were carried out with a home build system consisting of an Optical Parametric Oscillator (Opolette 355) pumped by a Nd:Yag laser used as an excitation source and the output of a Tungsten lamp (Bentham, IL 1) used as a broadband probe light source. The signals were detected by Si (Hamamatsu Photonics) or InGaAs (Hamamatsu Photonics) photodiodes. The photodiodes were housed in separate pre-amplifiers and connected to an electronic band pass filter (Costronics Electronics). An Oscilloscope (Tektronics, TDS220) synchronized with a trigger signal from the laser excitation source was used for data collection. In all measurements, the excitation pulses were set to 630 nm and had a nominal 20 ns pulse width. The samples were kept under a nitrogen atmosphere in a quartz cuvette. Optical cut-off filters and a monochromator were used to reduce laser scattering at the silicon photodiode from the excitation source and to adjust the probe light wavelength to 980 nm.

Femtosecond transient absorption spectroscopy was carried out using a commercially available transient absorption spectrometer, HELIOS (Ultrafast systems). Samples were excited with a pulse-train generated by an optical parametric amplifier, TOPAS (Light conversion). Both, the spectrometer

and the parametric amplifier were seeded with a 1 KHz, 800 nm, 100 femtosecond Solstice Ti:Sapphire regenerative amplifier (Newport Ltd). Samples were kept in a cuvette under Nitrogen atmosphere.

AUTHOR INFORMATION

Corresponding Authors

Stoichko D. Dimitrov (Stoichko.Dimitrov@swansea.ac.uk) and James R. Durrant
(j.durrant@imperial.ac.uk)

ACKNOWLEDGMENT

The authors would like to thank Florent Deledalle for the helpful discussions of non-geminate recombination dynamics and Safa Shoaee for measuring TEM images. We also thank the EPSRC (EP/I01927B/1 and EP/K011987/1) for funding. BCS acknowledges the National Research Fund of Luxembourg for financial support. This work is part-funded by the European regional Development Fund through the Welsh Government.

ABBREVIATIONS

GP geminate pair, PA photoinduced absorption, TEM transmission electron microscope, PL photoluminescence, NIR near infrared.

REFERENCES

- (1) Hu, H.; Jiang, K.; Yang, G.; Liu, J.; Li, Z.; Lin, H.; Liu, Y.; Zhao, J.; Zhang, J.; Huang, F.; Qu, Y.; Ma, W.; Yan, H. Terthiophene-Based D–A Polymer with an Asymmetric Arrangement of Alkyl Chains That Enables Efficient Polymer Solar Cells. *Journal of the American Chemical Society* **2015**.
- (2) Li, S.; Ye, L.; Zhao, W.; Zhang, S.; Mukherjee, S.; Ade, H.; Hou, J. Energy-Level Modulation of Small-Molecule Electron Acceptors to Achieve over 12% Efficiency in Polymer Solar Cells. *Advanced Materials* **2016**, *28*, 9423-9429.
- (3) Yang, Y.; Zhang, Z.-G.; Bin, H.; Chen, S.; Gao, L.; Xue, L.; Yang, C.; Li, Y. Side-Chain Isomerization on an n-type Organic Semiconductor ITIC Acceptor Makes 11.77% High Efficiency Polymer Solar Cells. *Journal of the American Chemical Society* **2016**, *138*, 15011-15018.
- (4) Mayer, A. C.; Toney, M. F.; Scully, S. R.; Rivnay, J.; Brabec, C. J.; Scharber, M.; Koppe, M.; Heeney, M.; McCulloch, I.; McGehee, M. D. Bimolecular Crystals of Fullerenes in Conjugated Polymers and the Implications of Molecular Mixing for Solar Cells. *Advanced Functional Materials* **2009**, *19*, 1173-1179.

- (5) Westacott, P.; Tumbleston, J. R.; Shoaee, S.; Fearn, S.; Bannock, J. H.; Gilchrist, J. B.; Heutz, S.; deMello, J.; Heeney, M.; Ade, H.; Durrant, J.; McPhail, D. S.; Stingelin, N. On the role of intermixed phases in organic photovoltaic blends. *ENERGY & ENVIRONMENTAL SCIENCE* **2013**, *6*, 2756-2764.
- (6) Bartelt, J. A.; Beiley, Z. M.; Hoke, E. T.; Mateker, W. R.; Douglas, J. D.; Collins, B. A.; Tumbleston, J. R.; Graham, K. R.; Amassian, A.; Ade, H.; Fréchet, J. M. J.; Toney, M. F.; McGehee, M. D. The Importance of Fullerene Percolation in the Mixed Regions of Polymer–Fullerene Bulk Heterojunction Solar Cells. *Advanced Energy Materials* **2013**, *3*, 364-374.
- (7) Collins, B. A.; Gann, E.; Guignard, L.; He, X.; McNeill, C. R.; Ade, H. Molecular Miscibility of Polymer-Fullerene Blends. *Journal of Physical Chemistry Letters* **2010**, *1*, 3160-3166.
- (8) Collins, B. A.; Li, Z.; Tumbleston, J. R.; Gann, E.; McNeill, C. R.; Ade, H. Absolute Measurement of Domain Composition and Nanoscale Size Distribution Explains Performance in PTB7:PC71BM Solar Cells. *Advanced Energy Materials* **2013**, *3*, 65-74.
- (9) Martens, T.; D’Haen, J.; Munters, T.; Beelen, Z.; Goris, L.; Manca, J.; D’Olieslaeger, M.; Vanderzande, D.; De Schepper, L.; Andriessen, R. Disclosure of the nanostructure of MDMO-PPV:PCBM bulk hetero-junction organic solar cells by a combination of SPM and TEM. *Synth. Met.* **2003**, *138*, 243-247.
- (10) Jamieson, F. C.; Domingo, E. B.; McCarthy-Ward, T.; Heeney, M.; Stingelin, N.; Durrant, J. R. Fullerene crystallisation as a key driver of charge separation in polymer/fullerene bulk heterojunction solar cells. *Chem. Sci.* **2012**, *3*, 485-492.
- (11) Mihailitchi, V. D.; Koster, L. J. A.; Blom, P. W. M.; Melzer, C.; de Boer, B.; van Duren, J. K. J.; Janssen, R. A. J. Compositional dependence of the performance of poly(p-phenylene vinylene):Methanofullerene bulk-heterojunction solar cells. *Advanced Functional Materials* **2005**, *15*, 795-801.
- (12) Veldman, D.; Ipek, O.; Meskers, S. C. J.; Sweelssen, J.; Koetse, M. M.; Veenstra, S. C.; Kroon, J. M.; van Bavel, S. S.; Loos, J.; Janssen, R. A. J. Compositional and electric field dependence of the dissociation of charge transfer excitons in alternating polyfluorene copolymer/fullerene blends. *Journal of the American Chemical Society* **2008**, *130*, 7721-7735.
- (13) Albrecht, S.; Vandewal, K.; Tumbleston, J. R.; Fischer, F. S. U.; Douglas, J. D.; Fréchet, J. M. J.; Ludwigs, S.; Ade, H.; Salleo, A.; Neher, D. On the efficiency of charge transfer state splitting in polymer:fullerene solar cells. *Advanced Materials* **2014**, *26*, 2533–2539.
- (14) Janssen, R. A. J.; Nelson, J. Factors Limiting Device Efficiency in Organic Photovoltaics. *Advanced Materials* **2013**, *25*, 1847-1858.
- (15) Scarongella, M.; De Jonghe-Risse, J.; Buchaca-Domingo, E.; Causa’, M.; Fei, Z.; Heeney, M.; Moser, J.-E.; Stingelin, N.; Banerji, N. A Close Look at Charge Generation in Polymer:Fullerene Blends with Microstructure Control. *Journal of the American Chemical Society* **2015**, *137*, 2908-2918.
- (16) Howard, I. A.; Mauer, R.; Meister, M.; Laquai, F. Effect of Morphology on Ultrafast Free Carrier Generation in Polythiophene:Fullerene Organic Solar Cells. *Journal of the American Chemical Society* **2010**, *132*, 14866-14876.
- (17) Gehrig, D. W.; Howard, I. A.; Sweetnam, S.; Burke, T. M.; McGehee, M. D.; Laquai, F. The Impact of Donor–Acceptor Phase Separation on the Charge Carrier Dynamics in pBTTT:PCBM Photovoltaic Blends. *Macromolecular Rapid Communications* **2015**, *36*, 1054-1060.
- (18) Bernardo, B.; Cheyns, D.; Verreet, B.; Schaller, R. D.; Rand, B. P.; Giebink, N. C. Delocalization and dielectric screening of charge transfer states in organic photovoltaic cells. *Nat Commun* **2014**, *5*.
- (19) Guilbert, A. A. Y.; Reynolds, L. X.; Bruno, A.; MacLachlan, A.; King, S. P.; Faist, M. A.; Pires, E.; Macdonald, J. E.; Stingelin, N.; Haque, S. A.; Nelson, J. Effect of Multiple Adduct Fullerenes on Microstructure and Phase Behavior of P3HT:Fullerene Blend Films for Organic Solar Cells. *ACS Nano* **2012**, *6*, 3868-3875.
- (20) Schroeder, B. C.; Huang, Z.; Ashraf, R. S.; Smith, J.; D’Angelo, P.; Watkins, S. E.; Anthopoulos, T. D.; Durrant, J. R.; McCulloch, I. Silaindacenodithiophene-based low band gap

polymers - the effect of fluorine substitution on device performances and film morphologies. *Advanced Functional Materials* **2012**, *22*, 1663-1670.

(21) Lin, J. D. A.; Mikhnenko, O. V.; Chen, J.; Masri, Z.; Ruseckas, A.; Mikhailovsky, A.; Raab, R. P.; Liu, J.; Blom, P. W. M.; Loi, M. A.; Garcia-Cervera, C. J.; Samuel, I. D. W.; Nguyen, T.-Q. Systematic study of exciton diffusion length in organic semiconductors by six experimental methods. *Materials Horizons* **2014**, *1*, 280-285.

(22) Tamai, Y.; Ohkita, H.; Benten, H.; Ito, S. Exciton Diffusion in Conjugated Polymers: From Fundamental Understanding to Improvement in Photovoltaic Conversion Efficiency. *The Journal of Physical Chemistry Letters* **2015**, *6*, 3417-3428.

(23) Armin, A.; Kassal, I.; Shaw, P. E.; Hamsch, M.; Stolterfoht, M.; Lyons, D. M.; Li, J.; Shi, Z.; Burn, P. L.; Meredith, P. Spectral Dependence of the Internal Quantum Efficiency of Organic Solar Cells: Effect of Charge Generation Pathways. *Journal of the American Chemical Society* **2014**, *136*, 11465-11472.

(24) Clarke, T. M.; Durrant, J. R. Charge Photogeneration in Organic Solar Cells. *Chemical Reviews* **2010**, *110*, 6736-6767.

(25) Dimitrov, S. D.; Durrant, J. R. Materials design considerations for charge generation in organic solar cells. *Chem. Mat.* **2014**, *26*, 616-630.

(26) Shoaee, S.; Subramaniyan, S.; Xin, H.; Keiderling, C.; Tuladhar, P. S.; Jamieson, F.; Jenekhe, S. A.; Durrant, J. R. Charge Photogeneration for a Series of Thiazolo-Thiazole Donor Polymers Blended with the Fullerene Electron Acceptors PCBM and ICBA. *Advanced Functional Materials* **2013**, *23*, 3286.

(27) Banerji, N. Sub-picosecond delocalization in the excited state of conjugated homopolymers and donor-acceptor copolymers. *Journal of Materials Chemistry C* **2013**, *1*, 3052-3066.

(28) Hestand, N. J.; Spano, F. C. The Effect of Chain Bending on the Photophysical Properties of Conjugated Polymers. *The Journal of Physical Chemistry B* **2014**, *118*, 8352-8363.

(29) Burke, T. M.; McGehee, M. D. How High Local Charge Carrier Mobility and an Energy Cascade in a Three-Phase Bulk Heterojunction Enable >90% Quantum Efficiency. *Advanced Materials* **2014**, *26*, 1923-1928.

(30) Ohkita, H.; Cook, S.; Astuti, Y.; Duffy, W.; Tierney, S.; Zhang, W.; Heeney, M.; McCulloch, I.; Nelson, J.; Bradley, D. D. C.; Durrant, J. R. Charge carrier formation in polythiophene/fullerene blend films studied by transient absorption spectroscopy. *Journal of the American Chemical Society* **2008**, *130*, 3030-3042.

(31) Foertig, A.; Kniepert, J.; Gluecker, M.; Brenner, T.; Dyakonov, V.; Neher, D.; Deibel, C. Nongeminate and geminate recombination in PTB7: PCBM solar cells. *Advanced Functional Materials* **2014**, *24*, 1306-1311.

(32) van Eersel, H.; Janssen, R. A. J.; Kemerink, M. Mechanism for Efficient Photoinduced Charge Separation at Disordered Organic Heterointerfaces. *Advanced Functional Materials* **2012**, *22*, 2700-2708.

(33) Gélinas, S.; Rao, A.; Kumar, A.; Smith, S. L.; Chin, A. W.; Clark, J.; van der Poll, T. S.; Bazan, G. C.; Friend, R. H. Ultrafast Long-Range Charge Separation in Organic Semiconductor Photovoltaic Diodes. *Science* **2014**, *343*, 512-516.

(34) Savoie, B. M.; Rao, A.; Bakulin, A. A.; Gelinas, S.; Movaghar, B.; Friend, R. H.; Marks, T. J.; Ratner, M. A. Unequal Partnership: Asymmetric Roles of Polymeric Donor and Fullerene Acceptor in Generating Free Charge. *Journal of the American Chemical Society* **2014**, *136*, 2876-2884.

(35) Sweetnam, S.; Graham, K. R.; Ngongang Ndjawa, G. O.; Heumüller, T.; Bartelt, J. A.; Burke, T. M.; Li, W.; You, W.; Amassian, A.; McGehee, M. D. Characterization of the Polymer Energy Landscape in Polymer:Fullerene Bulk Heterojunctions with Pure and Mixed Phases. *Journal of the American Chemical Society* **2014**, *136*, 14078-14088.

(36) Guilbert, A. A. Y.; Schmidt, M.; Bruno, A.; Yao, J.; King, S.; Tuladhar, S. M.; Kirchartz, T.; Alonso, M. I.; Goñi, A. R.; Stingelin, N.; Haque, S. A.; Campoy-Quiles, M.; Nelson, J.

Spectroscopic Evaluation of Mixing and Crystallinity of Fullerenes in Bulk Heterojunctions. *Advanced Functional Materials* **2014**, *24*, 6972-6980.

(37) Causa, M.; De Jonghe-Risse, J.; Scarongella, M.; Brauer, J. C.; Buchaca-Domingo, E.; Moser, J.-E.; Stingelin, N.; Banerji, N. The fate of electron-hole pairs in polymer:fullerene blends for organic photovoltaics. *Nature Communications* **2016**, *7*, 12556.

(38) Rance, W. L.; Ferguson, A. J.; McCarthy-Ward, T.; Heeney, M.; Ginley, D. S.; Olson, D. C.; Rumbles, G.; Kopidakis, N. Photainduced Carrier Generation and Decay Dynamics in Intercalated and Non-intercalated Polymer: Fullerene Bulk Heterojunctions. *ACS Nano* **2011**, *5*, 5635-5646.

(39) Reid, O. G.; Malik, J. A. N.; Latini, G.; Dayal, S.; Kopidakis, N.; Silva, C.; Stingelin, N.; Rumbles, G. The influence of solid-state microstructure on the origin and yield of long-lived photogenerated charge in neat semiconducting polymers. *Journal of Polymer Science Part B: Polymer Physics* **2012**, *50*, 27-37.

(40) Dimitrov, S. D.; Huang, Z.; Deledalle, F.; Nielsen, C. B.; Schroeder, B. C.; Ashraf, R. S.; Shoaee, S.; McCulloch, I.; Durrant, J. R. Towards optimisation of photocurrent from fullerene excitons in organic solar cells. *Energy & Environmental Science* **2014**, *7*, 1037-1043.

(41) Hedley, G. J.; Ward, A. J.; Alekseev, A.; Howells, C. T.; Martins, E. R.; Serrano, L. A.; Cooke, G.; Ruseckas, A.; Samuel, I. D. W. Determining the optimum morphology in high-performance polymer-fullerene organic photovoltaic cells. *Nat Commun* **2013**, *4*.

(42) Cook, S.; Furube, A.; Katoh, R.; Han, L. Y. Estimate of singlet diffusion lengths in PCBM films by time-resolved emission studies. *Chemical Physics Letters* **2009**, *478*, 33-36.

(43) Reid, O. G.; Pensack, R. D.; Song, Y.; Scholes, G. D.; Rumbles, G. Charge Photogeneration in Neat Conjugated Polymers. *Chem. Mat.* **2014**, *26*, 561-575.

(44) Dimitrov, S. D.; Wheeler, S.; Niedzialek, D.; Schroeder, B. C.; Utzat, H.; Frost, J. M.; Yao, J.; Gillett, A.; Tuladhar, P. S.; McCulloch, I.; Nelson, J.; Durrant, J. R. Polaron pair mediated triplet generation in polymer/fullerene blends. *Nat Commun* **2015**, *6*.

(45) Lioudakis, E.; Alexandrou, I.; Othonos, A. Ultrafast Dynamics of Localized and Delocalized Polaron Transitions in P3HT/PCBM Blend Materials: The Effects of PCBM Concentration. *Nanoscale Research Letters* **2009**, *4*, 1475-1480.

(46) Jiang, X. M.; Österbacka, R.; Korovyanko, O.; An, C. P.; Horovitz, B.; Janssen, R. A. J.; Vardeny, Z. V. Spectroscopic Studies of Photoexcitations in Regioregular and Regiorandom Polythiophene Films. *Advanced Functional Materials* **2002**, *12*, 587-597.

(47) Etzold, F.; Howard, I. A.; Mauer, R.; Meister, M.; Kim, T. D.; Lee, K. S.; Baek, N. S.; Laquai, F. Ultrafast exciton dissociation followed by nongeminate charge recombination in PCDTBT:PCBM photovoltaic blends. *Journal of the American Chemical Society* **2011**, *133*, 9469-9479.

(48) Jakowetz, A. C.; Böhm, M. L.; Zhang, J.; Sadhanala, A.; Huettner, S.; Bakulin, A. A.; Rao, A.; Friend, R. H. What Controls the Rate of Ultrafast Charge Transfer and Charge Separation Efficiency in Organic Photovoltaic Blends. *Journal of the American Chemical Society* **2016**, *138*, 11672-11679.

(49) Kaake, L. G.; Jasieniak, J. J.; Bakus, R. C.; Welch, G. C.; Moses, D.; Bazan, G. C.; Heeger, A. J. Photoinduced Charge Generation in a Molecular Bulk Heterojunction Material. *Journal of the American Chemical Society* **2012**, *134*, 19828-19838.

(50) Mihailitchi, V. D.; Koster, L. J. A.; Hummelen, J. C.; Blom, P. W. M. Photocurrent Generation in Polymer-Fullerene Bulk Heterojunctions. *Physical Review Letters* **2004**, *93*, 216601.

(51) Wojcik, M.; Tachiya, M. Geminate charge recombination with distance-dependent intrinsic reaction rate: Escape probability and its electric field effect. *Radiation Physics and Chemistry* **2005**, *74*, 132-138.

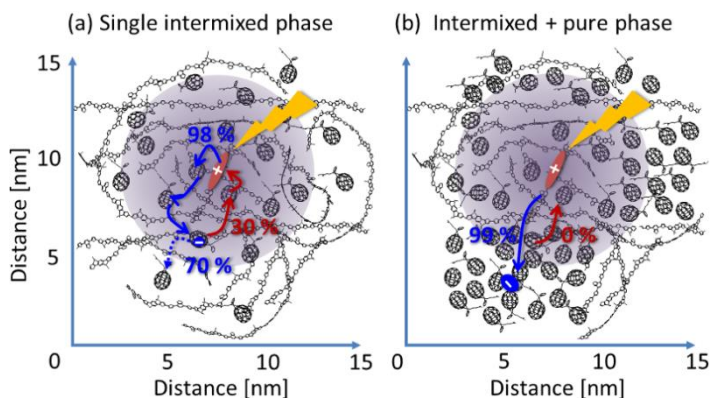
(52) Deibel, C.; Dyakonov, V. Polymer-fullerene bulk heterojunction solar cells. *Reports on Progress in Physics* **2010**, *73*, 096401.

(53) Nelson, J. Diffusion-limited recombination in polymer-fullerene blends and its influence on photocurrent collection. *Physical Review B* **2003**, *67*, 155209

- (54) Shuttle, C. G.; O'Regan, B.; Ballantyne, A. M.; Nelson, J.; Bradley, D. D. C.; Durrant, J. R. Bimolecular recombination losses in polythiophene: Fullerene solar cells. *Physical Review B* **2008**, *78*, 113201.
- (55) Melianas, A.; Etzold, F.; Savenije, T. J.; Laquai, F.; Inganäs, O.; Kemerink, M. Photo-generated carriers lose energy during extraction from polymer-fullerene solar cells. *Nature Communications* **2015**, *6*, 8778.
- (56) Clarke, T. M.; Ballantyne, A.; Shoaee, S.; Soon, Y. W.; Duffy, W.; Heeney, M.; McCulloch, I.; Nelson, J.; Durrant, J. R. Analysis of Charge Photogeneration as a Key Determinant of Photocurrent Density in Polymer: Fullerene Solar Cells. *Advanced Materials* **2010**, *22*, 5287-5291.
- (57) Keivanidis, P. E.; Clarke, T. M.; Lilliu, S.; Agostinelli, T.; Macdonald, J. E.; Durrant, J. R.; Bradley, D. D. C.; Nelson, J. Dependence of Charge Separation Efficiency on Film Microstructure in Poly(3-hexylthiophene-2,5-diyl):[6,6]-Phenyl-C61 Butyric Acid Methyl Ester Blend Films. *The Journal of Physical Chemistry Letters* **2010**, *1*, 734-738.
- (58) Banerji, N.; Cowan, S.; Leclerc, M.; Vauthey, E.; Heeger, A. J. Exciton Formation, Relaxation, and Decay in PCDTBT. *Journal of the American Chemical Society* **2010**, *132*, 17459-17470.
- (59) Etzold, F.; Howard, I. A.; Forler, N.; Cho, D. M.; Meister, M.; Mangold, H.; Shu, J.; Hansen, M. R.; Muellen, K.; Laquai, F. The effect of solvent additives on morphology and excited-state dynamics in PCPDTBT:PCBM photovoltaic blends. *Journal of the American Chemical Society* **2012**, *134*, 10569-10583.
- (60) Di Nuzzo, D.; Koster, L. J. A.; Gevaerts, V. S.; Meskers, S. C. J.; Janssen, R. A. J. The Role of Photon Energy in Free Charge Generation in Bulk Heterojunction Solar Cells. *Advanced Energy Materials* **2014**, *4*, 1400416-n/a.
- (61) Clarke, T. M.; Ballantyne, A. M.; Tierney, S.; Heeney, M.; Duffy, W.; McCulloch, I.; Nelson, J.; Durrant, J. R. Charge Photogeneration in Low Band Gap Polyselenophene/Fullerene Blend Films. *Journal of Physical Chemistry C* **2010**, *114*, 8068-8075.
- (62) Hawks, S. A.; Deledalle, F.; Yao, J.; Rebois, D. G.; Li, G.; Nelson, J.; Yang, Y.; Kirchartz, T.; Durrant, J. R. Relating Recombination, Density of States, and Device Performance in an Efficient Polymer:Fullerene Organic Solar Cell Blend. *Advanced Energy Materials* **2013**, *3*, 1201-1209.
- (63) Bakulin, A. A.; Dimitrov, S. D.; Rao, A.; Chow, P. C. Y.; Nielsen, C. B.; Schroeder, B. C.; McCulloch, I.; Bakker, H. J.; Durrant, J. R.; Friend, R. H. Charge-Transfer State Dynamics Following Hole and Electron Transfer in Organic Photovoltaic Devices. *Journal of Physical Chemistry Letters* **2013**, *4*, 209-215.
- (64) Li, W.; Roelofs, W. S. C.; Wienk, M. M.; Janssen, R. A. J. Enhancing the photocurrent in diketopyrrolopyrrole-based polymer solar cells via energy level control. *Journal of the American Chemical Society* **2012**, *134*, 13787-13795.
- (65) Dimitrov, S. D.; Bakulin, A. A.; Nielsen, C. B.; Schroeder, B. C.; Du, J. P.; Bronstein, H.; McCulloch, I.; Friend, R. H.; Durrant, J. R. On the Energetic Dependence of Charge Separation in Low-Band-Gap Polymer/Fullerene Blends. *Journal of the American Chemical Society* **2012**, *134*, 18189-18192.

The table of contents (TOC)

The morphology of the active layer of bulk-heterojunction organic solar cells on the nanometer lengthscale is shown to control the separation dynamics of photogenerated charges. Laser spectroscopic and structural data of films and devices reveal that subtle changes in the size of intermixed polymer-fullerene and pure fullerene domains influence strongly geminate charge recombination on the nanosecond timescale.



Keyword

Organic Solar Cells, Charge Photogeneration, Geminate Recombination, Morphology, Transient Absorption Spectroscopy

Hendrik Utzat^{1,2}, Stoichko D. Dimitrov^{1,3*}, Scot Wheeler¹, Elisa Collado-Fregoso¹, Pabitra Shakya Tuladhar¹, Bob C. Schroeder^{1,4}, Iain McCulloch¹ and James R. Durrant^{1,3*}

Charge Separation in Intermixed Polymer:PC70BM Photovoltaic Blends: Correlating Structural and Photophysical Length Scales as a Function of Blend Composition